Failure of extended-moment-equation approaches to describe ballistic transport in submicrometer structures

Maziar Nekovee,* Bernard J. Geurts,†‡ Henk M. J. Boots, and Martin F. H. Schuurmans
Philips Research Laboratories, P.O. Box 80 000, 5600 JA Eindhoven, The Netherlands
(Received 20 May 1991; revised manuscript received 30 October 1991)

Lower-order moment-equation models with a general nonlinear closing relation incorporating *a priori* ballistic and heating effects are studied numerically. Results for an n^+-n-n^+ diode show a reasonable agreement of these models with predictions obtained from the numerical solution to the corresponding Boltzmann equation in the nonballistic regime. In the predominantly ballistic regime, all lower-order models fail. A sketch of the parameter range in which these moment-equation models are valid is presented, based on a comparison of the predicted I-V characteristics. The conductance is inadequately described by all models, even in nonballistic cases, due to the high built-in potential, caused by the doping profile present in the device.

I. INTRODUCTION

The significant size reduction of semiconductor devices over the last few decades has prompted the need for device simulation models that do not presuppose equilibrium between electrons and phonons. Although it is often felt that Monte Carlo simulations[1] of electron transport in such devices will, in due time, be the most appropriate tool, presently workers in device simulation welcome descriptions that constitute extensions of the usual drift-diffusion approach. Many authors have proposed models that include the energy balance equation.[2] The most well-known recent model of this kind is the hydrodynamic model of Baccarani, and Wordeman[3] who adopt a Fourier law for the heat flux.[4] In this paper, we present a systematic hierarchy of moment equations, as well as corresponding closing relations for the approximate description of transport properties of semiconducting submicrometer structures, closely following earlier work by Bringer and Schön[5] and Portengen, Boots, and Schuurmans.[6] We solve the moment equations numerically for a test case, the n^+-n-n^+ diode, for a wide range of parameter values and compare predictions of various moment-equation models with those obtained from a full solution to the corresponding Boltzmann equation.

The transport of electrons in semiconducting submicrometer structures is characterized by both hot and ballistic electrons, as well as large gradients in, e.g., the electron density and the electric field locally. Reduction of typical sizes and the use of high-mobility materials in device applications cause these far-from-equilibrium effects to become even more pronounced and result in the failure of conventional device simulation models, e.g., the "drift-diffusion" and the "hydrodynamic" models. We introduce a truncated expansion of the Boltzmann distribution function around a local reference state, which generates systematically a general class of (nonlinear) closing relations.[5] A proper choice of the local reference state allows for an *a priori* inclusion of ballistic and heating effects without having to resort to additional empirical considerations related to the definition of the closing relation.[6] The four-moment-equation models obtained in this way are highly nonlinear and the combination with Poisson's equation calls for the use of an extended Scharfetter-Gummel scheme in the numerical treatment.[7–9]

From the four-moment-equation models we obtain the electron density, the current density, the kinetic-energy density, the kinetic-energy-density current, and the electron temperature. The main result of the paper is the I-V characteristic of our four-moment model(s) in comparison with the results from the drift-diffusion and hydrodynamic model(s) and the exact results directly obtained from the corresponding Boltzmann equation. These results indicate that all lower-order moment-equation models give reasonably accurate predictions in the nonballistic regime, i.e., for small relaxation times and/or wide structures. However, in the predominantly ballistic regime these predictions become inaccurate; all lower-order models show large errors in the predicted transport properties if the parameters are outside a certain region. The truncation order of the moment model has only a small effect on this parameter region, i.e., increasing this order does not lead to a significant extension of the region for which the predictions are useful. The error in the predictions of the moment models increases very rapidly and in a manner which is not very sensitive to the truncation order of the model as the parameters approach the ballistic regime. This suggests that it is not possible to treat predominantly ballistic transport phenomena with any low-order system of moment equations. This is the main conclusion of this paper. In addition, the large built-in potentials found in these structures cause the failure of all moment models to correctly predict the conductance, even in the nonballistic regime, i.e., departure from the local equilibrium reference state is described rather poorly.

Of course, the use of the relaxation-time approximation of the collision integral in the Boltzmann equation implies an exaggeration of ballistic effects.[10] However,

we feel that even when using more realistic scattering terms, similar discrepancies will be found for predominantly ballistic transport. Roughly speaking, if the product of relaxation time and maximal drift velocity in the diode is on the order of the width of the n-type region or larger, the moment model predictions deviate significantly from those of the corresponding Boltzmann equation.[11] In essence, this is due to the fact that the distribution function develops a sharp high-velocity ballistic peak next to a "bell-shaped" near-equilibrium distribution at lower velocities within the structure.[10,12,13] Hence, it can no longer be expected to be representable by any small number of moments, e.g., a single typical velocity and temperature scale. Conversely, in the nonballistic regime, such a high-velocity peak is absent and the essential structure of the distribution function can quite well be captured with a small number of typical scales and/or moments. The virtue of extended-moment-equation models lies mainly in the fact that a larger number of different moments are predicted, not so much in the extension of the parameter range over which these models give reasonably accurate predictions of the actual moments. Increasing the truncation order leads to an extension of this parameter region; however, it does not give an essential increase in the sense that strong ballistic effects come within reach. As will be shown, these extended models are numerically not much more involved in one-dimensional simulations, when compared to drift-diffusion models. At the same time, these models are capable of predicting a large number of relevant physical quantities whereas the related computational effort is much smaller than that required when solving the corresponding Boltzmann equation. We will indicate the parameter range for which these moment models remain valid and can be usefully applied to the n^+-n-n^+ diode.

In the next section we describe our moment approach to the Boltzmann equation and discuss in some detail the derivation of the closing relations. Then we present the numerical results obtained for a wide range of parameter values and compare the different moment models. We also show the corresponding results obtained from the full Boltzmann equation and hence sketch a range of parameters for which the moment approaches are valid. Finally, we give a summary of our findings.

II. EXTENDED-MOMENT APPROACHES TO BOLTZMANN'S EQUATION

We derive a systematic hierarchy of moment equations and closing relations approximating the corresponding Boltzmann transport equation, closely following Bringer and Schön[5] and Portengen, Boots, and Schuurmans.[6] We show that an expansion of the distribution function around a generalized "Maxwellian" reference function in Hermite polynomials leads to a set of closing relations in which ballistic and heating effects are included *a priori*.

The stationary Boltzmann equation governs the electron distribution function $f(r,v)$ and in one spatial and one velocity dimensions reads[10]

$$[v\partial_r - E(r)\partial_v]f(r,v) = -\frac{1}{\tau}[f(r,v)-f_0(r,v)] , \tag{1}$$

where we adopt the parabolic-band approximation and assume a constant-relaxation-time representation (with rate τ) for the collision term. We use scaled variables; position r and velocity v are measured in units r_0 (the Debye length) and v_0 (the thermal velocity), respectively where

$$r_0 = \left[\frac{\epsilon k_B T_0}{e^2 M_{\rm ref}}\right]^{1/2} ; \quad m^* v_0^2 = k_B T_0 , \tag{2}$$

with the understanding that k_B is Boltzmann's constant, T_0 the lattice temperature, ϵ the permittivity, e the unit of charge, m^* the effective mass, and $M_{\rm ref}$ a reference particle density in the system. Also, f_0 is considered the distribution function describing local equilibrium, and both f and f_0 are taken in units $M_{\rm ref}/v_0$. The electric field E is measured in units $E_0 \equiv (m^* v_0^2)/(e r_0)$ and is determined by Poisson's equation, which can be expressed in the above notation as

$$\partial_{rr}\Psi(r) = M_0(r) - C(r); \quad E = -\partial_r \Psi , \tag{3}$$

where $C(r)$ describes the doping profile and M_0 the particle density, in units $M_{\rm ref}$. An n^+-n-n^+ diode is represented by the following doping profile:

$$C(r) = \begin{cases} C_+, 0 \le r \le d_1, d_2 \le r \le l \\ C_-, d_1 < r < d_2 , \end{cases} \tag{4}$$

with l denoting the total length of the diode and $d_1 < d_2$. In the following, we will use $M_{\rm ref} = C_+$.

Physically relevant information is usually expressed in terms of velocity moments of the distribution function, i.e., the mth moment M_m is defined as $M_m \equiv \langle v^m \rangle$, $m = 0,1,2,\ldots$. The set of moments $\{M_m(r)\}$ can readily be shown to obey, using the Boltzmann equation (1)

$$d_r M_{m+1} + mEM_{m-1} = -\frac{1}{\tau}\{M_m - M_{m,0}\} . \tag{5}$$

We will use the local equilibrium (Maxwellian) distribution

$$f_0(r,v) \equiv \frac{M_0(r)}{\sqrt{2\pi}} \exp\left[-\frac{v^2}{2}\right] , \tag{6}$$

which implies that the reference moments $\{M_{m,0}\}$ are given by

$$M_{2m,0} = M_0 \prod_{j=1}^{m} (2j-1); \quad M_{0,0} = M_0 , \tag{7}$$

and $M_{2m+1,0} = 0$. One observes that the mth moment is governed, in part, by the spatial derivative of the $(m+1)$th moment. Hence, a closing relation must be postulated expressing a higher-order moment in terms of lower-order moments. Once such a closing relation is obtained, the system of Eqs. (5) becomes finite and can be treated numerically.

We next derive the closing relations. A systematic way of generating a class of closing relations is by truncating an expansion of the distribution function f. Consider the following expansion of f:

$$f(r,v)=\frac{e^{-\xi^2/2}}{\sqrt{2\pi}}\sum_{j=0}^{\infty} f_j(r)H_j(\xi)\ , \tag{8}$$

where $\{H_j\}$ are Hermite polynomials[14] and $\xi\equiv[v-v_1(r)]/v_2(r)$. Thus, we propose to expand f around a Maxwellian distribution [viz. the factor $\exp(-\xi^2/2)$] with the option of including a suitably transformed and/or scaled velocity through the introduction of v_1 and v_2. A judicious choice of v_1 and v_2 can improve the accuracy of a truncating approximant to f without increasing the order of truncation. As will be shown, choosing v_1 to be the scaled drift velocity and v_2^2 the electron temperature relative to the lattice temperature generates an expansion in which f_1 and f_2 are identically zero. Since $v^m f$ can now be explicitly integrated with respect to v, the expansion functions $\{f_j(r)\}$ can be expressed as linear combinations of the moments $\{M_m\};m=0,1,\ldots,j$ and the functions v_1 and v_2. Hence, truncating the above expansion at some order n by putting $f_n=0$ renders a relation between M_n and $\{M_j\};j=0,1,\ldots,n-1$ which will be used as the closing relation. The first few closing relations obtained in this way are

$$\begin{aligned}
&f_1=M_1-p_1(v_1)M_0=0, \quad \text{for } n=1\ ;\\
&f_2=M_2-2p_1(v_1)M_1-p_2(v_1,v_2)M_0=0, \quad \text{for } n=2\ ;\\
&f_3=M_3-3p_1(v_1)M_2-3p_2(v_1,v_2)M_1\\
&\qquad -p_3(v_1,v_2)M_0=0, \quad \text{for } n=3\ ;\\
&f_4=M_4-4p_1(v_1)M_3\\
&\qquad -6p_2(v_1,v_2)M_2-4p_3(v_1,v_2)M_1\\
&\qquad +p_4(v_1,v_2)M_0=0, \quad \text{for } n=4\ ;
\end{aligned} \tag{9}$$

where

$$\begin{aligned}
p_k(v_1,v_2)=&-p_1(v_1)p_{k-1}(v_1,v_2)\\
&-(k-1)v_2^2p_{k-2}(v_1,v_2)
\end{aligned} \tag{10}$$

for $k=3,4,5,\ldots,$ with $p_1(v_1)=v_1$

and

$$p_2(v_1,v_2)=v_2^2-v_1^2\ .$$

We will not pursue the structure of these closing relations as expressed above but concentrate on the fourth-order closing relations which will be the highest order considered in this paper, as an example. One has, written out in full,

$$\begin{aligned}
M_4=&4v_1M_3+6(v_2^2-v_1^2)M_2+4v_1(v_1^2-3v_2^2)M_1\\
&-(v_1^4-6v_2^2v_1^2+3v_2^4)M_0\ .
\end{aligned} \tag{11}$$

The functions v_1 and v_2 are arbitrary, but the structure of Eq. (9) suggests that a proper choice of these functions renders lower-order expansion functions identically zero. Hence, it is expected that the accuracy of the expansion can be improved without having to increase the truncation order. Putting $v_2=1$ and $v_1=0$ implies expanding f around a pure Maxwellian distribution and results in

$$M_4=6M_2-3M_0\ , \tag{12}$$

whereas taking $v_1=M_1/M_0$ renders $f_1\equiv 0$, and the corresponding closing relation in this case reads

$$M_4=4v_1M_3+6(1-v_1^2)M_2-3(1+2v_1^2-v_1^4)M_0\ . \tag{13}$$

This corresponds to an expansion of f around a "drifted" Maxwellian, i.e., the velocity is corrected with the drift velocity of the electrons. Evidently, the function v_2 can now be used to render $f_2\equiv 0$ as well through

$$v_2^2\equiv\frac{M_2M_0-M_1^2}{M_0^2}\ , \tag{14}$$

which results in the closing relation

$$M_4=4v_1M_3+6(v_2^2-v_1^2)M_2-3[2v_2^4-(v_2^2-v_1^2)^2]M_0\ . \tag{15}$$

This corresponds to expanding f around a "scaled and drifted" Maxwellian, i.e., velocity is corrected with the drift velocity and scaled with the local temperature. The above derivation can readily be specialized to lower-order models ($n=2,3$). For example, in the $n=2$ case (drift-diffusion models), the expansion around a pure Maxwellian results in $M_2=M_0$, whereas an expansion around a drifted Maxwellian yields $M_2=(v_1^2+1)M_0$, with $v_1=M_1/M_0$. These models have been studied numerically as well and will be discussed in Sec. III.

The above clearly shows that a judicious choice of the "transformation" functions v_1 and v_2 has the potential to result in improved expansions of f. The consequence, however, is that the closing relations become less transparent and nonlinear. Moreover, the ansatz for f is an expansion around a local scaled and/or drifted Maxwellian reference state and, hence, we may certainly expect some improvements of the predictions for "nearby" situations. However, we have no guarantee as to the accuracy of the various predictions for situations far away from equilibrium.

III. MODEL PREDICTIONS FOR AN n^+-n-n^+ DIODE

We first present numerical results obtained for the moment-equation models introduced in the preceding section. Special attention will be paid to transport properties and their dependence on the truncation order in the model and material parameters, such as the relaxation time and the width of the n-type region. Then we compare these predictions with those obtained by solving the full Boltzmann equation (1), concentrating, in particular, on the I-V characteristics.

We consider the four-moment models based upon expansion around an equilibrium Maxwellian [closing relation (12)], a drifted Maxwellian [closing relation (13)], and a drifted and heated Maxwellian [closing relation (15)], together with the drift diffusion as well as the hydrodynamic model. Our test structure will be an n^+-n-n^+ GaAs diode, with $m^*=0.069m_e$ (m_e being the

electron rest mass), $\epsilon_r = 12.5$, an n-type-region width of 10^{-7}–10^{-6} m and a total length l of 10^{-6}–10^{-5} m. Doping concentrations are taken as $C_+ = 10^{24}$ m^{-3} and $C_- = 2\times10^{21}$ m^{-3}. Different relaxation times will be used in the range 10^{-13}–10^{-14} s. We calculate the electron density (n), the current density (j), kinetic-energy density (K), kinetic-energy-density current (Q), and the "quadratic kinetic-energy density" (R). These are related to the dimensionless moments introduced above by

$$n = M_{\rm ref} M_0; \quad j = -ev_0 M_{\rm ref} M_1; \quad K = \tfrac{1}{2} m^* v_0^2 M_{\rm ref} M_2, \tag{16}$$

$$Q = \tfrac{1}{2} m^* v_0^3 M_{\rm ref} M_3; \quad R = \tfrac{1}{4}(m^*)^2 v_0^4 M_{\rm ref} M_4 . \tag{17}$$

We also consider the electron temperature (T_e) and the drift velocity (v_d), which are defined by

$$T_e \equiv T_0 \frac{M_2 M_0 - M_1^2}{M_0^2}; \quad v_d \equiv v_0 \frac{M_1}{M_0} . \tag{18}$$

A brief description of the numerical procedure used to treat the moment-equation models is given in the Appendix; see also Ref. 9.

We first turn to the results of the four-moment model based upon an expansion around a pure Maxwellian distribution, i.e., with Eq. (12) as a closing relation. These results form the basis with which corresponding results based on the other four-moment models, the drift-diffusion models, the hydrodynamic model, as well as the full Boltzmann equation, will be compared below. In Figs. 1–4 we show n, K, Q, and R, respectively, displaying the influence of variations in the applied voltage V.

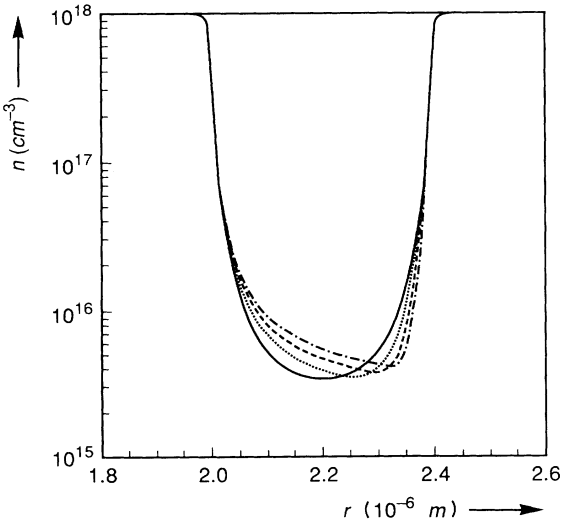

FIG. 1. The electron density (n) as a function of position for the four-moment model with Eq. (12) as closing relation, showing the influence of applying a voltage. We used $V=0$ V (full curve); $V=0.15$ V (dotted curve); $V=0.3$ V (dashed curve), and $V=0.45$ V (chain-dotted curve). This labeling of the curves also applies for Figs. 2–4. In these calculations we used an n^+-n-n^+ diode with a width $d=0.4\times10^{-6}$ m and a total length of $l=4.4\times10^{-6}$ m. The relaxation time $\tau=1.0\times10^{-13}$ s.

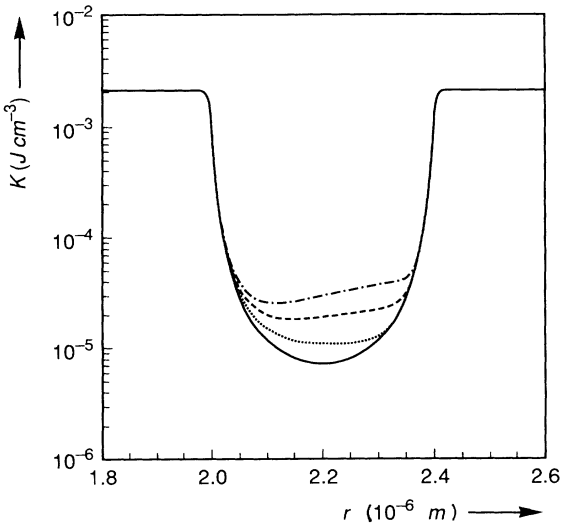

FIG. 2. The kinetic-energy density (K) as a function of position for the same parameters and model as in Fig. 1.

The electron density n becomes asymmetric due to the applied voltage and the minimum gradually shifts to the high-voltage region. The kinetic-energy density K exhibits more or less opposite behavior; moreover, K builds up a small overshoot near the high-voltage region. The kinetic-energy-density current Q shows two distinct peaks near the doping steps which become larger as V is increased. Finally, the quadratic-kinetic-energy density R displays qualitatively the same dependence on V as K. The electron temperature T_e exhibits a cooling effect related to the potential barrier near the first doping interface and a heating of the electrons inside the doping profile as shown in Fig. 5. Notice that at sufficiently high voltages this model predicts negative electron temperatures, in conflict with physical reality. This reflects the fact that the truncated approximate-distribution function becomes negative within the structure. The predicted temperature profiles are physically unacceptable at

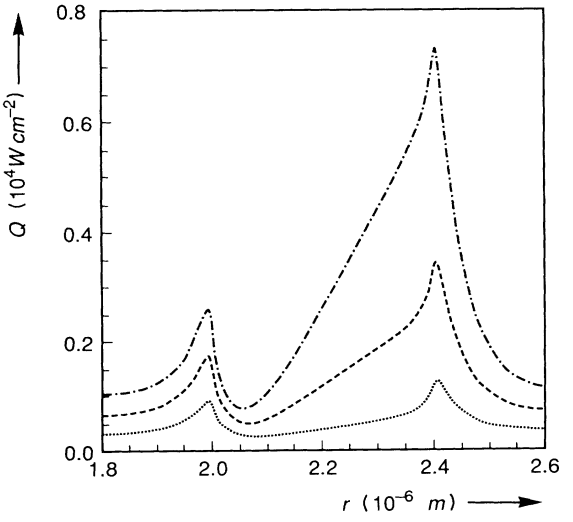

FIG. 3. The kinetic-energy-density current (Q) as a function of position for the same parameters and model as in Fig. 1.

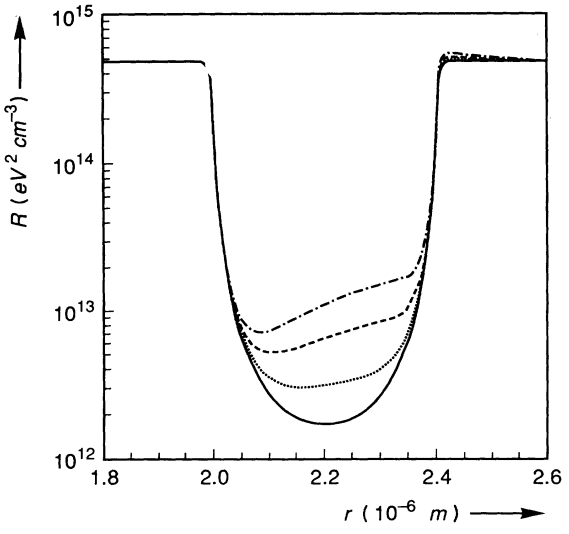

FIG. 4. The quadratic-kinetic-energy density (R) as a function of position for the same parameters and model as in Fig. 1.

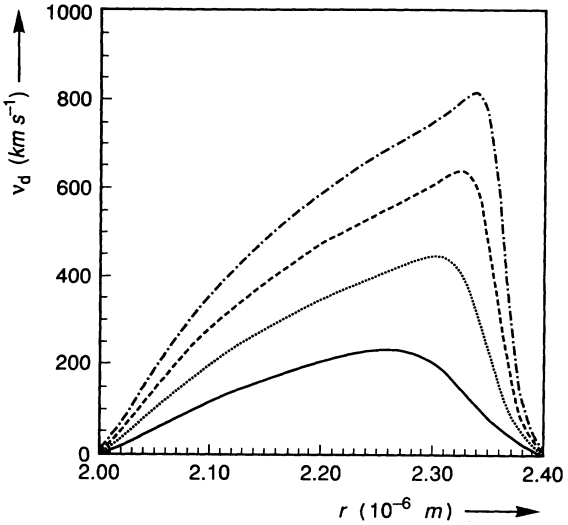

FIG. 6. The drift velocity as predicted by the four-moment model with Eq. (12) as a closing relation with parameters as in Fig. 5.

sufficiently high voltages. In Fig. 6 the drift velocity (v_d) is shown. The maximal drift velocity increases as the applied voltage is increased; the electrons are extremely accelerated within the n-type region.

We also studied the influence of varying the electron relaxation time τ and the width of the n-type region. A decrease in the width d and/or an increase in the relaxation time, corresponding to enhanced ballistic effects, results in an amplification of the effects observed above. At the same applied voltage the moments differ significantly more from their corresponding local equilibrium state. The qualitative behavior of the momenta as a function of position, however, remains the same. It will be shown later on that the same variations in the parameters τ and d yield a poorer agreement between the moment equation predictions and the results obtained from direct solution of the Boltzmann equation. Roughly speaking, as τv_d is of the order of d, ballistic effects tend to dominate the transport and the lower-order moment-equation models fail. A high-velocity ballistic peak develops in the distribution function f and cannot be accurately represented by a small number of typical moments.

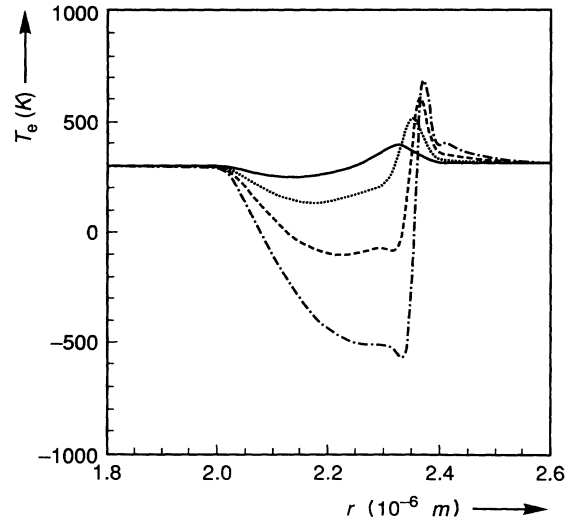

FIG. 5. The electron temperature as predicted by the four-moment model with Eq. (12) as closing relation at applied voltages of $V=0.15$ V (full curve); $V=0.3$ V (dotted curve); $V=0.45$ V (dashed curve), and $V=0.6$ V (chain-dotted curve). We used $\tau=1.7\times10^{-13}$ s, and the values for d and l are as in Fig. 1.

The use of the nonlinear closing relations (13) or (15), i.e., expansion based upon a drifted and a drifted and heated Maxwellian, respectively, does not lead to any significant changes in the predicted moments at low applied voltages. As one might expect from the extended ansatz to f used in these cases, the predictions of these "nonlinear" models are improved in the low-voltage regime, but this improvement is, however, quite small. The predictions of the nonlinear models [Eqs. (13) and (15)] compare almost perfectly with those presented in Figs. 1–6, in the low-voltage regime. However, as V is increased sufficiently, both these models reach a critical point at which the solution branches terminate. This is due to the fact that the partial derivative of the closing relation with respect to M_0 approaches zero at some point within the device and the set of governing differential equations degenerates in the sense that there is no longer an equation containing $d_r M_0$. Thus, the electron density is no longer continuously differentiable. One may introduce jump conditions to go beyond this point.[15] We, however, did not pursue this approach, but rather limited the applied voltage such that this critical situation was not reached. For applied voltages slightly lower than the critical value, the electron density starts to show up a sharp "kink" at the position at which the partial derivative of the closing relation with respect to M_0 reaches its maximum. Again, an increase in τ and/or a decease in d amplifies these effects and the limiting applied voltages become quite low in the strong ballistic re-

gime; so the nonlinear models fail to give any predictions at more realistic applied voltages for ballistic devices. This is illustrated in Fig. 7, in which we show the critical voltages (V_c) of the nonlinear models (13) and (15) for two different devices, as a function of the relaxation time τ. If $V > V_c$, no solution exists. As d decreases and/or τ increases, the critical voltage rapidly decreases, rendering V_c quite small in ballistic situations. Moreover, the predictions of the nonlinear models start to deviate appreciably from those based on model (12) only in a very small region of voltages below V_c. Everywhere else in the parameter space, the predictions almost perfectly agree with those presented in Figs. 1–6. We return to this momentarily, in Figs. 8 and 9. Typically, for applied voltages $V < 0.95V_c$ all four-moment models introduced yield essentially the same predictions. For a more detailed discussion, see Ref. 9. Roughly speaking, if ballistic effects start to dominate heating effects, these critical situations are reached. As an example, the drifted Maxwellian drift-diffusion model, as given below Eq. (15), terminates exactly when v_1 becomes equal to one. If this happens, the corresponding closing relation is such that the derivative with respect to M_0 is 0 and the equations no longer contain a differential equation governing M_0. The condition $v_1 = 1$ is readily interpreted. It arises if $M_1 = M_0$ at some point in the device, i.e., if the drift velocity (v_d) is equal to the thermal velocity (v_0) defined in Eq. (2).

We next turn to a comparison of the kinetic-energy-density current Q, the electron temperature T_e, and the electron density n as predicted by the above four-moment models, the hydrodynamic model, and the full Boltzmann equation. Then we proceed with a discussion of the corresponding I-V characteristics to obtain a sketch of the parameter region for which moment-equation models as used in this paper can be usefully applied. In Fig. 8, we show the various predictions for Q as a function of position. Notice that already at this low applied voltage the differences between the hydrodynamic and four-moment models are quite large. Also, all four-moment models give roughly the same predictions, apart from small improvements in the n-type region, when using the nonlinear models. All moment models predict excessively sharp peaks in Q, though the discrepancies in the four-moment models are not as large as in the hydrodynamic model. The use of four moments rather than three, as in the hydrodynamic model, leads in this instance to a slightly improved agreement between the moment predic-

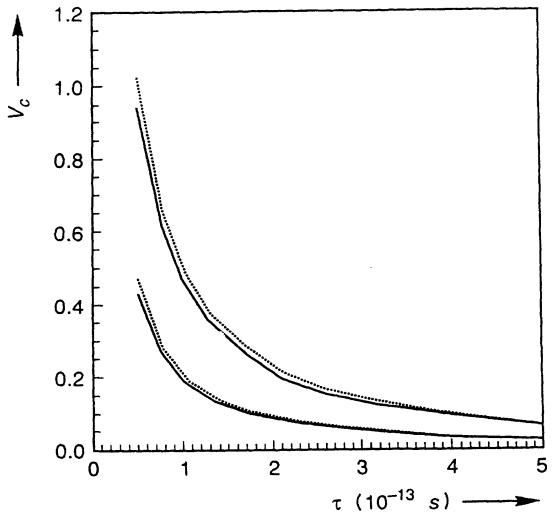

FIG. 7. The critical voltage V_c as a function of the relaxation time τ for the four-moment model closed by Eq. (13) (full curve) and Eq. (15) (dashed curve) at $l = 4.4 \times 10^{-6}$ m and $d = 0.4 \times 10^{-6}$ m (lower two lines); $d = 0.8 \times 10^{-6}$ m (upper two lines).

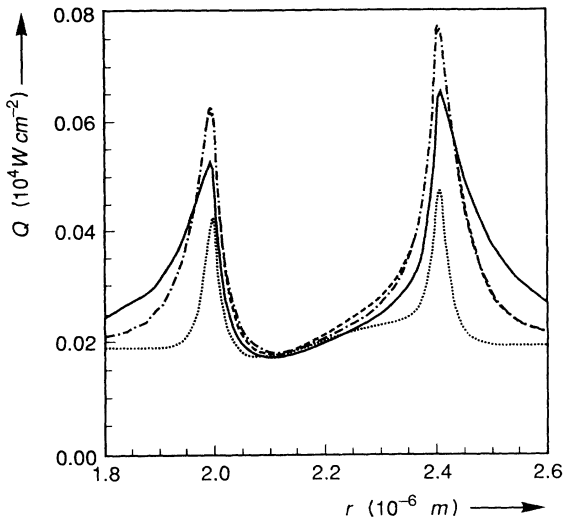

FIG. 8. The kinetic-energy-density current (Q) as a function of position comparing the four-moment models and the prediction of the hydrodynamic model with the Boltzmann predictions. We used an applied voltage $V = 0.1$ V and parameters as in Fig. 1. The Boltzmann result is shown as a full curve, the hydrodynamic result as a dotted curve, and the four-moment model with Eq. (12) as a dashed curve, with Eq. (13) as a chain dotted curve, and with Eq. (15) as a long-dashed curve.

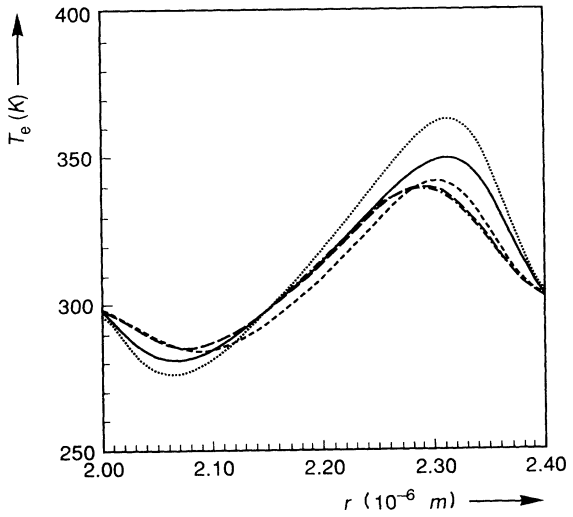

FIG. 9. The electron temperature T_c as a function of position with the same parameters as in Fig. 7 and similar curve labeling.

tions and the Boltzmann results. However, turning to the electron temperature (T_e) in Fig. 9 indicates that all models perform with roughly the same accuracy. It is seen that the hydrodynamic model overestimates the cooling and heating effects, whereas the four-moment models underestimate these effects. The results presented in Figs. 8 and 9 correspond to a comparison of all models at one parameter setting. We also studied the effects of varying τ, d, and V. As mentioned before, an increase in τ and/or a decrease in d enhances ballistic effects and the discrepancies shown in Figs. 8 and 9 become larger, although they remain of a similar nature as far as underestimating and overestimating the corresponding Boltzmann-equation results is concerned. The effect of increasing the applied voltage also corresponds to decreased accuracy in the predictions. In Fig. 10 we plotted the electron density (n) at a low and a high voltage, comparing the Boltzmann equation results with the (linear) drift-diffusion and four-moment model results. Other moment models give similar results and the overall resemblance is quite good in all these cases, although the logarithmic scale used here is somewhat deceiving. Further comparison of the results indicates, on the whole, a fair agreement between the various predictions of the even-order moments (i.e., n, K, and R), even in the ballistic regime, and a much less accurate representation of the odd order moments.

We proceed with a comparison of the I-V characteristics of the various moment models and the corresponding Boltzmann-equation results. These results are of most direct practical use and are shown in Fig. 11. If τ is low, all models give almost equally accurate results, whereas in strong ballistic situations, all models deviate considerably from the Boltzmann results. Increasing the truncation order from two (drift-diffusion) to four does extend the parameter region in which the predictions deviate by

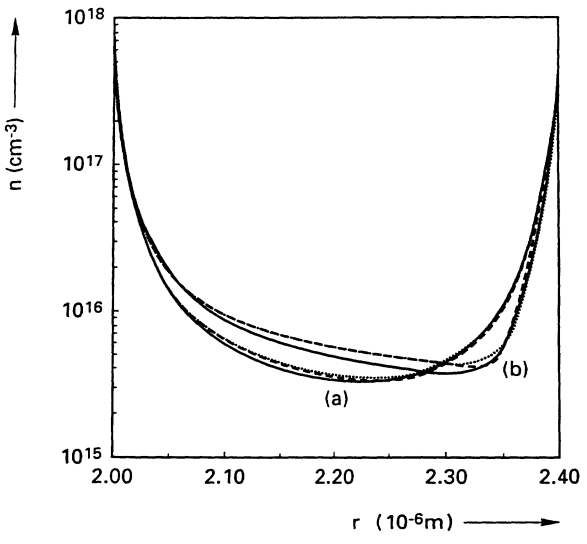

FIG. 10. The electron density n as a function of position at $\tau=2.9\times10^{-13}$ s and $V=0.1$ V (case a); $V=0.5$ V (case b). The Boltzmann results are shown as full curves, the drift-diffusion results as dotted curves, and the four-moment results as dashed curves. Parameters are taken as in Fig. 1.

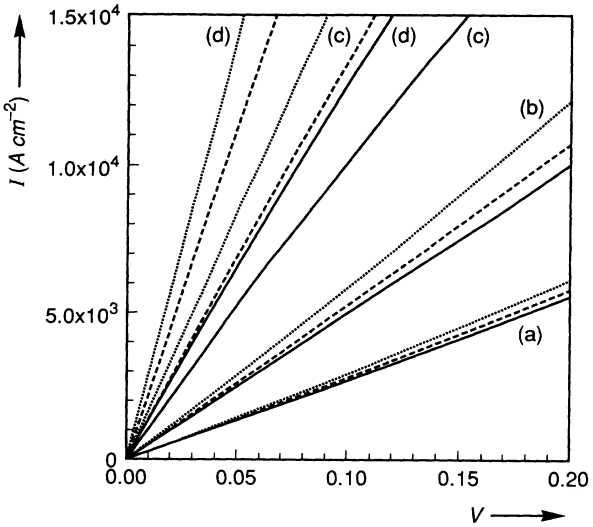

FIG. 11. Comparison of the I-V characteristics as predicted by the different linear-moment models with the corresponding Boltzmann results showing the influence of variations of the relaxation time τ, keeping d fixed to 0.4×10^{-6} m. The Boltzmann results are represented by the full curves, the drift-diffusion results by the dotted curves, and the four-moment models by the dashed curves. In the calculations τ was varied between $\tau=5\times10^{-14}$ s (labeled a); 1×10^{-13} s (labeled b); 2.9×10^{-13} s (labeled c); and 5×10^{-13} s (labeled d). The other parameters are as in Fig. 1.

less than (say) 10%. It does not, however, extend this region into the predominantly ballistic regime. It was observed that the I-V predictions of the linear and nonlinear two- and four-moment models agree quite well with each other in the entire parameter region studied and hence the results for the nonlinear models are not shown here. For details we refer to Ref. 9. Further, the hydrodynamic model gives the most accurate results for relatively small relaxation times. At higher relaxation times it fails to give any predictions at realistic applied voltages due to instabilities related to drift velocity approaching the thermal velocity.[15] In order to show the effects of varying the width of the n-type region in the diode, we plotted the current as a function of width in Fig. 12. A similar observation can be made here; as d is decreased, i.e., ballistic effects are amplified, the agreement between the moment models and the Boltzmann models decreases. As a measure of the "ballisticity" in the system one may introduce $B\equiv\tau v_{d,\max}/d$ with $v_{d,\max}$, the maximal drift velocity in the system. Comparing current predictions as a function of B shows that $I_B/I_m\sim-\log_{10}(B)$ for large enough B. Here I_B denotes the current as predicted by the Boltzmann equation and I_m the corresponding moment equation result. Typically, for B smaller than $\frac{1}{2}$, the ratio I_B/I_m is constant and smaller than 1 to close approximation, and this ratio decreases rapidly as B increases above $\frac{1}{2}$.[11] This implicitly sketches the parameter region in which moment-equation models can be usefully applied. Apparently none of these models extends into the strong ballistic regime and additional approximation schemes should be used in order to

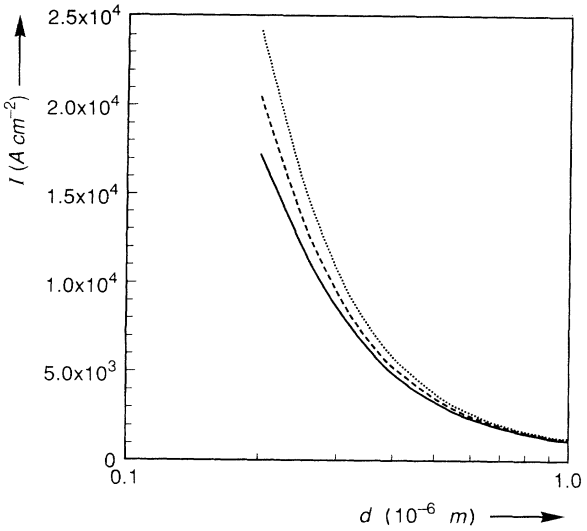

FIG. 12. Comparison of the predicted current showing the influence of variation in the width of the n-type region, keeping $\tau=1\times10^{-13}$ s at an applied voltage of $V=0.1$ V. The full curve represents the Boltzmann results, the dotted curve the drift diffusion results, and the dashed curve the four-moment results.

generate models that cover the full range of different behavior. Moreover, all moment models predict the conductance dI/dV as $V\rightarrow0$ incorrectly, even in nonballistic cases, partly due to the high built-in potential found in submicrometer structures. The latter high potential implies that even at low applied voltages far from equilibrium, situations are generated with great ease locally, for which the previous results have shown poor agreement between the moment-model predictions and the Boltzmann-equation results.

IV. CONCLUDING REMARKS

We compared a systematic hierarchy of moment-equation models with the corresponding Boltzmann equation. The *a priori* inclusion of ballistic and heating effects was studied and shown to yield somewhat improved agreement between the moment predictions and the Boltzmann results at low applied voltages, in accordance with the improvement of the approximation around local equilibrium. However, these ballistic and heating effects were shown to give rise to nonlinear closing relations and the occurrence of critical voltages beyond which no unique solution exists. Comparison with lower-order moment models showed an improved agreement with the Boltzmann results when increasing the truncation order from two (drift-diffusion) to four. However, the results also indicated that this improvement does not really imply that strong ballistic effects can be adequately described with any low-order moment-equation model. In the event that τv_d becomes of the order of d, all moment models fail quite abruptly. A further comparison with the hydrodynamic model, which uses a Fourier law to relate the heat flux to the electron temperature, showed that the latter model gives surprisingly accurate predictions of the I-V characteristics, although its predictions cannot also be translated into the strong ballistic regime. In addition, the prediction of T_e and Q by the hydrodynamic model are again quite inaccurate, even at low applied voltages in the "mildly" ballistic regime ($\tau\approx1\times10^{-13}$ s and $d\approx0.4\times10^{-6}$ m). The use of an abrupt doping profile is not essential in these model calculations. We also considered smooth but rapidly varying profiles and obtained similar results. The numerical effort required in solving these models is only moderately increased when increasing the truncation order, in one dimension, though in higher dimensional applications the higher-order moment-equation models do give rise to much more involved numerical problems.

ACKNOWLEDGMENT

The helpful and stimulating discussions with Professor Dr. G. Schön at Delft University, The Netherlands, are gratefully acknowledged by the authors.

APPENDIX: NUMERICAL SOLUTION METHOD

We formulate the four-moment model explicitly and sketch the discretization scheme used. It will become clear that this scheme is a natural generalization of the Scharfetter-Gummel[7–9] scheme frequently used in drift-diffusion models. It is particularly fit to treat the exponentially varying components of the solution. Then we sketch the total algorithm generating the final self-consistent solution.

In the stationary state, the four-moment model reads

$$d_{rr}\Psi=M_0-C\ , \tag{A1}$$

$$d_rM_1=0\ , \tag{A2}$$

$$d_rM_2+EM_0=-\frac{1}{\tau}M_1\ , \tag{A3}$$

$$d_rM_3+2EM_1=-\frac{1}{\tau}\{M_2-M_0\}\ , \tag{A4}$$

$$d_rM_4+3EM_2=-\frac{1}{\tau}M_3\ , \tag{A5}$$

where d_r denotes differentiation with respect to r and the closing relation is expressed as

$$M_4=\mathcal{F}(M_0,M_1,M_2,M_3)\ . \tag{A6}$$

Notice that the local-equilibrium reference state implies that we may add an arbitrary function of M_1 to this closing relation without changing the predictions for M_0,M_1,M_2, and M_3. With the use of this closing relation we eliminate M_4 from the model given by (A1)–(A5) and thus obtain a closed system from which M_0,M_1,M_2, and M_3 can be determined. Obviously, this only holds if $\partial_{M_0}\mathcal{F}\neq0$, i.e., for systems of equations that are Lipschitz. Upon eliminating M_4 from Eq. (A5) using the closing relation (A6), a term $\partial_{M_0}\mathcal{F}d_rM_0$ appears. Hence, if $\partial_{M_0}\mathcal{F}\neq0$ the resulting set of equations (A2)–(A5) constitute four ordinary differential equations governing M_0,M_1,M_2, and M_3. If $\partial_{M_0}\mathcal{F}=0$ at some point in the device, however, the resulting equations no longer con-

tain $d_r M_0$ and no unique differentiable solution exists. The boundaries will be treated as Ohmic contacts, i.e.,

$$\Psi(0)=0; \quad \Psi(l)=V , \tag{A7}$$

$$M_0(0)=M_0(l)=M_2(0)=M_2(l)=1 , \tag{A8}$$

where V denotes the scaled applied voltage.

The above system of equations is highly nonlinear and due to the (large and abrupt) steps in the doping profile (typically $C_- \ll C_+$), the solution for M_0 and M_2 shows large local variations near the "interfaces" of the doping steps. Hence, it is necessary to devise a discretization scheme which accurately follows these large exponential variations in order to keep the numerical effort limited. Also, in view of the boundary conditions for M_0 and M_2, it is useful to eliminate M_1, M_3 from the problem formally and to derive an equivalent set of three second-order equations.

The procedure for doing this and taking the exponential variations into account proceeds in a few steps. It is based on solving Eqs. (A3) and (A5) locally analytically around a mesh point in which E, M_1, M_3, and the partial derivatives of $\mathcal{J}$ with respect to the moments are approximated as constant over a small region around a mesh point. These analytic solutions for M_0 and M_2 contain two integration constants and the assumed values of M_1 and M_3 as parameters. Thus, by a lengthy calculation, it is possible to find the latter two values such that the local approximations for M_0 and M_2 exactly agree with the desired solution at the mesh points. One thus obtains expressions for the values of M_1 and M_3 at the mesh points $r_{i+1/2}$ in terms of M_0 and M_2 at r_i and r_{i+1}. Here $\{r_i\}$ denotes a covering mesh and we introduced $r_{i+1/2} \equiv (r_i + r_{i+1})/2$. Finally, treating the remaining Eqs. (A2) and (A4) by a standard finite difference scheme gives three-point relations for M_0 and M_2 at the mesh points. It is then a standard matter to solve for the moments at a given electric field and an initial guess for the moments. The electric field E shows sharp peaks near the doping steps and in order to have an accurate evaluation of the equations the calculation mesh was chosen such that $M_0 - C$ was approximately equally distributed, resulting in correspondingly small mesh intervals near the doping steps. Iteration between these equations and the Poisson equation, gradually updating all moments, results in the desired self-consistent solution. Details of the derivation of the above scheme, as well as an analysis of its performance, will be published elsewhere.[9] The main point is that sharp local variations in the solution have been taken into account fully by the above local analytic solution method. It generates a finite difference scheme which is "tuned" to the above system of equations. It is straightforward to customize this treatment to lower-order moment models, thus arriving at the well-known Scharffetter-Gummel scheme in the case of the drift-diffusion model and the scheme as reported in Ref. 3 for the hydrodynamic model with a Fourier law as closing relation for the heat flow. Notice that the above procedure is only valid if $\partial_{M_0} \mathcal{J}$ does not change sign as a function of position. If this does happen the corresponding moment model has a finite solution branch, i.e., in particular, the voltage range for which the model has a unique solution is limited since the system of equations is no longer Lipschitz beyond a certain voltage.

---

*Present address: Theoretical Physics 1, Katholieke Universiteit Nijmegen, Toernooiveld, 6520 ED Nijmegen, The Netherlands.

†Present address: Twente University, Department of Applied Mathematics, P.O. Box 217, 7500 AE Enschede, The Netherlands.

‡To whom correspondence should be addressed.

[1]P. J. Price, in *Semiconductors and Semimetals,* edited by R. K. Willardson and A. C. Beer (Academic Press, New York, 1979), Vol. 14, p. 249; C. Jacoboni and l. Reggiani, Rev. Mod. Phys. **55**, 645, (1983); C. Moglestue, IEEE Trans. Comput. Aided Des. **CAD-5**, 326 (1986); K. Hess, *Advanced Theory of Semiconductor Devices* (Prentice-Hall, Englewood Cliffs, NJ, 1988); M. V. Fischetti and S. E. Laux, Phys. Rev. B **38**, 9721 (1988); E. Sangiorgi, B. Riccó, and F. Venturi, IEEE Trans. Comput. Aided Des. **CAD-7**, 259 (1988).

[2]R. Stratton, Phys. Rev. **126**, 2002 (1962); R. K. Cook and J. Frey, IEEE Trans. Electron Devices **ED-29**, 970 (1982); C. T. Wang, Solid-State Electron. **28**, 783 (1985); W. Hänsch and M. Miura-Mattausch, J. Appl. Phys. **60**, 650 (1986); E. Schöll and W. Quade, J. Phys. C **20**, L871 (1987); B. Meinerzhagen and W. L. Engl, IEEE Trans. Electron. Devices **ED-35**, 689 (1988); E. M. Azoff, J. Appl. Phys. **64**, 2439 (1988).

[3]G. Baccarani and M. R. Wordeman, Solid-State Electron. **28**, 407 (1985).

[4]K. Blotekjaer, IEEE Trans. Electron Devices **ED-17**, 38 (1970).

[5]A. Bringer and G. Schön, J. Appl. Phys. **64**, 2447 (1988).

[6]T. Portengen, H. M. J. Boots, and M. F. H. Schuurmans, J. Appl. Phys. **68**, 2817 (1990).

[7]D. L. Scharfetter and H. K. Gummel, IEEE Trans. Electron Devices **ED-16**, 64 (1969).

[8]S. Selberherr, *Analysis and Simulation of Semiconductor Devices* (Springer-Verlag, Berlin, 1984).

[9]B. J. Geurts (unpublished).

[10]H. U. Baranger and J. W. Wilkins, Phys. Rev. B **36**, 1487 (1987).

[11]B. J. Geurts, M. Nekovee, H. M. J. Boots, and M. F. H. Schuurmans, Appl. Phys. Lett. **59**, 1743 (1991).

[12]B. J. Geurts, J. Phys. C **3**, 9447 (1991).

[13]B. J. Geurts (unpublished).

[14]*Handbook of Mathematical Functions,* edited by M. Abramowitz and I. A. Stegun (Dover, New York, 1972).

[15]C. L. Gardner, J. W. Jerome, and D. J. Rose, IEEE Trans. Comput. Aided Des. **CAD-8**, 501 (1989).